22nd Australasian Fluid Mechanics Conference AFMC2020
Brisbane, Australia, 6–10 December 2020
DOI: 10.14264/uql.2020.175.

A numerical simulation of an under-expanded jet issued from a prototype injector

M. R. Yosri[1], M. Talei[1], R. L. Gordon[1], M. J. Brear[1] and J. S. Lacey[2]

[1]Department of Mechanical Engineering,
The University of Melbourne, Parkville 3010, Australia.

[2] Department of Mechanical Engineering,
KU Leuven, 3001 Leuven, Belgium

Abstract

The injection of methane from a prototype outward opening injector into a quiescent, non-reacting Constant Volume Chamber (CVC) is modelled by using Large-Eddy Simulation (LES). Two different injector geometries are investigated: the first includes the full, internal geometry of the injector and the second uses a shortened version of the injector with a region upstream of the injection point. The effects of the injector's internal geometry on downstream flow characteristics such as the jet penetration length and spreading angle are examined. The LES results are validated against high-speed schlieren imaging experiments. It has been shown that when the pressure loss within the injector is taken into account, a reasonable agreement is achieved for the downstream flow features of the full injector geometry.

Keywords
Large-Eddy Simulation (LES); Constant Volume Chamber (CVC); Schlieren; Under-expanded gaseous jet; Direct Injection (DI)

Introduction

Alternative fuels such as Compressed Natural Gas (CNG) can lead to a significant reduction of emissions from the transport sector. This fuel has favourable properties compared with conventional fuels, including low Particulate Matter (PM), nitrogen oxide (NO_x), and CO_2 emissions, and high antiknock resistance [1]. CNG use in SI engines may therefore have several benefits over conventional fuels.

Spark Ignited (SI) CNG engines can use two different injection methodologies, Port Fuel Injection (PFI) and Direct Injection (DI). In PFI, CNG is injected into the intake manifold, and a premixed fuel-air mixture enters the combustion chamber. In DI, CNG is injected directly into the combustion chamber. Using CNG DI increases the volumetric efficiency and power output and therefore decreases CO_2 emissions [2].

CNG DI requires higher rail pressures compared with those of PFI to achieve a sufficient mass flow rate and fast air/fuel mixing [3]. The nozzle pressure ratio (NPR), the ratio of the rail pressure to the chamber pressure, is an important parameter to characterise gas injection. Increasing the NPR transitions the gas jet from a subsonic jet to a moderately under-expanded and eventually to a highly under-expanded jet [4]. CNG DI engines typically feature rail pressures around 20 bar whereas the chamber pressure is approximately 0.4-4 bar at different injection timing. As a result, moderately to highly under-expanded jets are generally present in CNG DI engines. Complex flow features such as shock waves and expansion fans presents in these kinds of gaseous jets [5].

The gas injector geometry can play a dominant role in the air/fuel mixing process. Gaseous injectors were initially developed using the Gasoline Direct Injection (GDI) concept with an inward opening valve which can have single or multi cylindrical holes. These kinds of gas injectors suffer from various issues such as leakage and undesired negative pressure difference within the injector. The new generation of gaseous DI injectors with an outward opening poppet valve has overcome the leakage issues since they can be sealed by the cylinder pressure. [6]. In this type of injector, the flow within the injector encounter the poppet valve as a "bluff body" and due to this, discontinuities such as boundary layer separation could happen at the tip of the injector [7]. Further investigation is required to understand the air/fuel mixing process of an under-expanded jet resulting from an outward opening injector considering these complex features.

Computational fluid dynamics (CFD) have been used to investigate the effect of the injector geometry on the gas dynamics of the external flow. Kim *et al.* showed that adding a shroud around the poppet valve directed the supersonic flow towards the centre of the gaseous jet axis and formed a "bell-shaped" jet, downstream of the poppet valve [8]. Baratta *et al.* showed that the diameter of the injector holes can affect the mass flow rate and the exit momentum of the jet [9]. They also observed that poppet valve motion led to pressure wave propagation within the injector and affect the mass flow rate. They concluded that considering the valve lift profile is required in the numerical simulation to replicate the experimental results at the early stage of the gaseous jet development. Deshmukh *et al.* demonstrated that neglecting the transient motion of the poppet valve could cause inaccurate prediction of the gaseous jet development up until the full-opening of the injector [7].

Previous numerical studies on outward opening injectors only considered a part of the injector close to the nozzle tip to perform the simulations. To include the effects of the internal injector geometry, the maximum valve lift and inlet pressure were altered to match the simulated mass flow rate with the experimental results [7]. Also, high fidelity simulations such as Large-Eddy Simulation (LES) is required to capture the salient features of the under-expanded jet and discontinuities like boundary layer separation [10, 11]. Considering the valve lift profile is essential to have a correct prediction of the jet development in the early stages of a LES as well.

The objective of this study is to perform LES of methane injection from a prototype outward opening injector using the full injector geometry. Another LES study will consider a shorter version of the injector with the injection pressure obtained by measuring the pressure loss from the former simulation. The external flow features of these two simulations will be compared with each other. A comparison with the experimental schlieren images from Lacey *et al.* [12] will also be presented.

Injection Hardware and Operating Conditions

A prototype injector from Continental is employed for this study [13]. Figure 1 shows the cross-sectional view of the injector, with the coloured flow path. The injector consists of two main parts; an internal, inward opening "cold" valve actuated by a solenoid and an external, outward opening "hot" valve that is spring-actuated. The "hot valve" is opened by the pressure difference between the fuel in the injector body and the chamber gas into which it is injected.

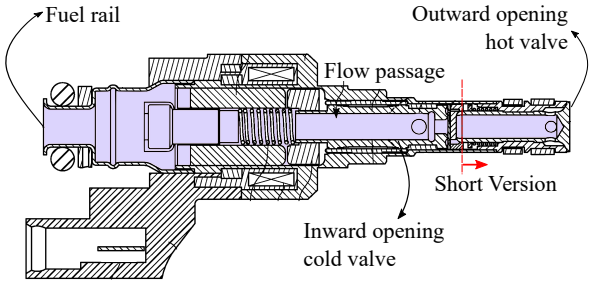

Figure 1. Sectional view of the prototype DI CNG injector, indicating the coloured flow path and location of the short version, inward and outward opening valves [13].

Lacey *et al.* [12] injected methane as a CNG surrogate into a quiescent, non-reacting Constant Volume Chamber (CVC). In this study, the results for a CVC pressure of 1 *bar* and a temperature of 298 K were used for comparison. The fuel rail pressure was kept constant at 20 *bar*.

Valve Lift Measurements

The valve lift profile was measured experimentally by using the high speed images. In this experiment, the injector was pulsed for 2 *ms* and movies were taken at 30,000 frames per second (fps) with a physical scaling of approximately 25 μm per pixel. The movies were then post-processed to find the edge of the poppet valve and measure its movement with time.

Figure 2 shows the results for the valve lift profile with the CVC pressure of 1 *bar* and a temperature of 298 K for both the fuel rail and CVC. A 700 μs delay exists from sending the signal to the solenoid to the opening of the valve. The valve height keeps increasing for approximately 300 μs until the valve approaches its maximum lift. The poppet valve then bounces till reaches a stable condition after approximately 500 μs. When the signal is switched off, the valve gradually closes and experiences some fluctuations before completely closing.

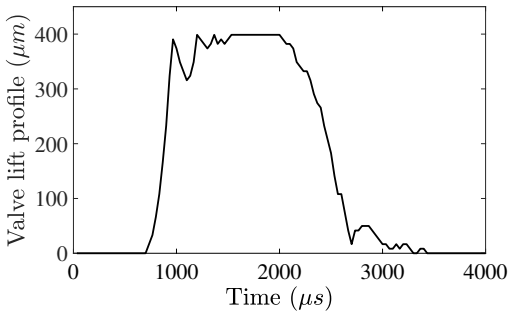

Figure 2. Experimental valve lift profile with the rail pressure of 20 *bar*, a CVC pressure of 1 *bar* and a temperature of 298 K in the fuel rail and CVC.

Numerical Methods

CONVERGE CFD software package [14] is employed to perform a three dimensional LES. A non-iterative implicit scheme entitled as the Pressure Implicit with the Splitting of Operators (PISO) algorithm, was used to solve the governing equations [15]. The time step was calculated based on the maximum of the Courant Friedrich Lewy (CFL) number (convection, diffusion and Mach number). The time step varied from 10^{-9} to 5×10^{-8} s with the 2 *ms* injection duration.

A one equation non-viscosity based Dynamic Structure model was used to model the Sub-Grid Scale stress (SGS) tensor [16]. Further details on the governing equations and the selection of constants are addressed in [14]. In order to save computational cost, the Adaptive Mesh Refinement (AMR) algorithm [14] was used. The AMR algorithm was activated based on the sub-grid field of a velocity and methane mass fraction (Y_{CH_4}) . The base grid size of this study was 1 mm, and the finest grid size was 0.03 mm. In addition, the total number of cells was limited to 15,000,000 overall mesh size. Further details on the applied AMR algorithm can be found in [14].

Two different cases were modelled in this study. In the first case, the full injector geometry with the rail pressure of 20 *bar*, CVC pressure of 1 *bar* and the temperature of 298 K was modelled. The pressure at the location of the short version ("hot valve", see Figure 1) was then recorded with respect to time. The results indicated that the pressure reaches from 1 *bar* initial condition to a 12 *bar* quasi-steady-state condition (from 300 to 2000 μs). Therefore, a constant pressure of 12 *bar* was used as the inlet pressure for the second, shorter injector geometry.

In both cases, the Reynolds number inside the injector varied from 10^5 to 10^6, and the Knudsen number was in the order of 0.01. Therefore, velocity slip boundary conditions were applied to the adiabatic walls within the injector [3]. At the tip of the poppet wall, as boundary layer separation occurs, no-slip boundary condition was applied. After the "cold valve" is closed, it takes more than 500 μs for the "hot valve" to completely close (see Figure 2). Hence, in both cases, the initial pressure and temperature of the "hot valve" are assumed to be the same as the CVC chamber condition. The injector was assumed to be filled with methane o nly. The chamber condition included the pressure and temperature of 1 *bar* and 298 K respectively, and the nitrogen mass fraction, $Y_{N_2} = 1$.

Results and Discussions

Lacey *et al.* [12] provided results for the axial and radial penetration of the jet, characterising the jet development. To find the radial penetration, a cone angle 5 *mm* downstream of the injector, called the jet spreading angle, was reported. The axial penetration was recorded 500 μs After the Start of the Injection (ASOI) until the width of the imaging window (37 *mm*). The jet spreading angle was calculated from 500 to 2000 μs ASOI when the jet cone angle was developed and reached the quasi-steady state condition. To find these two parameters in the numerical simulations, the iso-surface of the methane mass fraction $Y_{CH_4} = 0.01$ was used to find the jet boundary, penetration length, and spreading angle.

Figure 3 shows the comparison of the jet penetration length for the two cases with the experimental results. The case with the full injector geometry has a very good agreement with the experimental results (less than 6% difference at each time instant). The jet penetration length for the short injector case shows an over-prediction of around 7% up to where the injector is fully opened. This is because the pressure at the inlet of the short injector, is still below 12 *bar* before approximately 300 μs ASOI.

Once the injector is fully open, the difference between the results with the full injector and the short version is less than 5%. The experimental results shown by circles in Figure 4 are ensemble-averaged over the 50 injection events [12]. The standard deviation error bars for the mean values are about $\pm 5\%$ which is close to the difference between the results of short and full injectors for the penetration length.

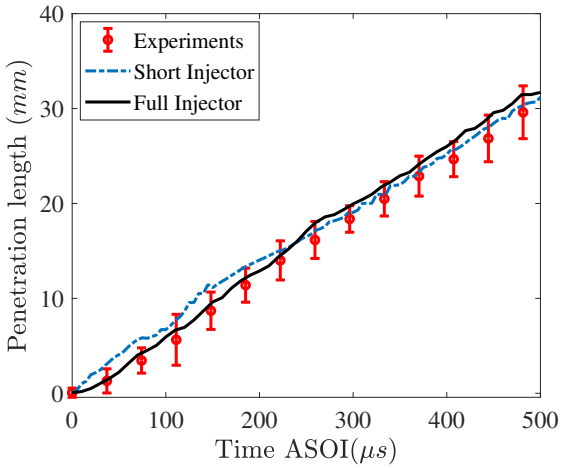

Figure 3. Comparison of the experimental and numerical results for the jet penetration length.

Table 1 presents the results for the time averaged jet spreading angle (cone angle) at quasi steady state condition (i.e. 500 to 2000 μs ASOI). The time averaged cone angle of the full injector shows a very good agreement (less than 1%) with the experimental result. Meanwhile, there are less than 3% difference between the results from the short version of the injector and experiments. The experimental jet spreading angle results indicate a standard deviation of $\pm 5\%$ across different injection events and the 3% difference is in the range of experimental uncertainties.

Table 1. Time averaged jet spreading angle at quasi steady state condition

Case	Averaged Cone Angle	Difference with Experiment (%)
Experiment	109°	-
Full Injector	108°	0.92
Short Injector	106°	2.75

Figure 4 illustrates the transient development of the methane mass fraction at the mid-Y-Z plane for the two LES cases. At 200 μS ASOI, as the pressure inside the "hot valve" has not reached 12 *bar*, the overall shape of the jet for the short version is different from the full injector case. Meanwhile, at 400 μS ASOI the jet collapsed and formed a single jet in both cases. At later times, 400 and 600 μS, the overall shapes of the jet for both cases are similar.

Conclusions

Large-eddy simulations (LESs) of direct methane injection into a Constant Volume Chamber (CVC) from a hollow-cone injector were performed. Two different cases that used the full internal geometry and a short version of the injector with a CVC pressure of 1 *bar*, and a temperature of 298 K were discussed and compared with schlieren images of Lacey *et al.* [12].

It was shown that modelling the internal geometry increases the accuracy of the simulation results. However, using the simulated pressure loss inside the full injector to set up the boundary conditions for the short version of the injector can also lead to a reasonable agreement with the experimental results in terms of the external flow characteristics.

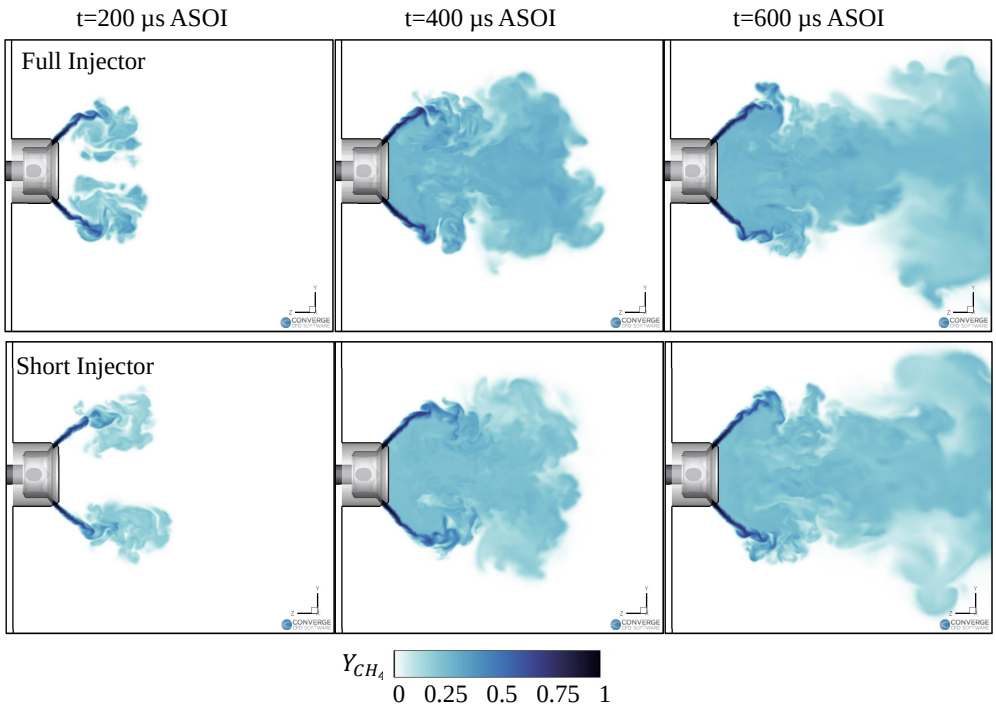

Figure 4. Methane mass fraction at the mid Y-Z plane during the injection process.

Acknowledgements

This research was supported by the Australian Research Council (ARC) [LP160100339] and the Ford Motor Company. Mohsen Talei acknowledges the support of the ARC through the DECRA Fellowship (DE180100416). We also would like to thank Continental for providing the prototype DI CNG injector hardware.

References

[1] Engerer, H. and Horn, M. (2010). Natural gas vehicles: An option for Europe. *Energy Policy*, 38 (2), 1017–1029.

[2] Ferrera, M. (2017). Highly efficient natural gas engines. *SAE International*, Paper No. 2017-04-0059.

[3] Hamzehloo, A. and Aleiferis, P. G. (2016). Numerical modelling of transient under-expanded jets under different ambient thermodynamic conditions with adaptive mesh refinement. *International J. of Hydrogen Energy*, 41 (15), 6544–6566.

[4] Donaldson, R. S. and Snedeker, C. (1971). A study of free jet impingement. *Journal of Fluid Mechanics*, 45 (2), 281–319.

[5] Yosri, M. R., Lacey, J. S., Talei, M. Gordon, R. L. and Brear, M. J. (2018). Development of a Verification Methodology for Large-Eddy Simulation of Under-expanded Natural Gas Jets. *In proc. of 21st Australasian Fluid Mechanics Conference*, Adelaide.

[6] Husted, H. L., Karl, G., and Weber, C. (2014). Direct Injection of CNG for Driving Performance with Low CO_2. *in 23rd Aachen Colloquium Auto-mobile and Engine Technology*, 126(3), Aachen, 82–850.

[7] Deshmukh, A. Y., Bode, M., Falkenstein, T., Khosravi, M., van Beber, D., Klass, M., Schroeder, W, and Pitch, H (2019). Simulation and modelling of direct gas injection through poppet-type outwardly-opening injectors in Internal Combustion Engines *Natural Gas Engines. Energy, Environment, and Sustainability. Springer, Singapore*, 65–115.

[8] Kim, G., Kirkpatrick, A. and Mitchell, C. (2004). Computational Modeling of Natural Gas Injection in a Large Bore Engine *Journal of Engineering for Gas Turbines and Power*,126 (3), 656–664.

[9] Baratta, M., Catania, A. E. and Pesce, F. C. (2011). Multidimensional Modelling of Natural Gas Jet and Mixture Formation in Direct Injection Spark Ignition Engines—Development and Validation of a Virtual Injector Model. *Journal of Fluids Engineering*, 133 (4), 41304–41314.

[10] Rutland C. J, (2017). Large-eddy simulations for internal combustion engines – a review. *International Journal of Engine Research*, 12 (5), 421–451.

[11] Vuorinen, V., Wehrfritz, A. Duwig, C. and Boersma, B.J. (2014). Large-eddy simulation on the effect of injection pressure and density on fuel jet mixing in gas engines . *Fuel*, 120, 241–250.

[12] Lacey, J. S., Meulemans, M., Poursadegh, F., Brear, M., Petersen, P., Kramer, U., Smith, A., Hornby, M., Cosby, D. and Czimmek, P. (2019). An Optical and Numerical Characterisation of Directly Injected Compressed Natural Gas Jet Development at Engine-Relevant Conditions. *SAE International*, Paper No. 2019-01-0294.

[13] Hornby, M., Husslein, K., Schule, H., Heukenroth, C., Klemp, T., Komischke, T. and Gerlach, T. (2015). Gas direct injector with reduced leakage. *US Patent*, No. US9453486B1.

[14] Richards, K. J., Senecal, P. K., and Pomraning, E. (2019). CONVERGE 2.4, Convergent Science, Madison, WI.

[15] Issa, R. I., Gosman, A. D., and Watkins, A. P. (1986). The computation of compressible and incompressible recirculating flows by a non-iterative implicit scheme. *Journal of Computational Physics*, 62 (1), 66–82.

[16] Pomraning, E. and Rutland, C. J. (2002). Dynamic One-Equation Nonviscosity Large-Eddy Simulation Model. *AIAA*, 40 (4), 689–701.